Molecular Biology of the Cell
Vol. 19, 1162–1173, March 2008

Distinct Chromatin Modulators Regulate the Formation of Accessible and Repressive Chromatin at the Fission Yeast Recombination Hotspot *ade6-M26*

Kouji Hirota,*† Ken-ichi Mizuno,‡ Takehiko Shibata,*§ and Kunihiro Ohta*†

*Shibata Distinguished Senior Scientist Laboratory, RIKEN Discovery Research Institute, Wako-shi, Saitama 351-0198, Japan; †Department of Life Sciences, Graduate School of Arts and Sciences, The University of Tokyo, Komaba, Tokyo 153-8902, Japan; ‡Genome Damage and Stability Centre, University of Sussex, Brighton BN1 9RQ, United Kingdom; and §Division of Molecular and Cellular Physiology, International Graduate School of Arts and Sciences, Yokohama City University, Yokohama, Kanagawa 230-0045, Japan

Submitted April 25, 2007; Revised December 17, 2007; Accepted January 4, 2007
Monitoring Editor: Wendy Bickmore

Histone acetyltransferases (HATs) and ATP-dependent chromatin remodeling factors (ADCRs) regulate transcription and recombination via alteration of local chromatin configuration. The *ade6-M26* allele of *Schizosaccharomyces pombe* creates a meiotic recombination hotspot that requires a cAMP-responsive element (CRE)-like sequence *M26*, the Atf1/Pcr1 heterodimeric ATF/CREB transcription factor, the Gcn5 HAT, and the Snf22 SWI2/SNF2 family ADCR. Chromatin alteration occurs meiotically around *M26*, leading to the activation of meiotic recombination. We newly report the roles of other chromatin remodeling factors that function positively and negatively in chromatin alteration at *M26*: two CHD-1 family ADCRs (Hrp1 and Hrp3), a Spt-Ada-Gcn5 acetyltransferase component (Ada2), and a member of Moz-Ybf2/Sas3-Sas2-Tip60 family (Mst2). Ada2, Mst2, and Hrp3 are required for the full activation of chromatin changes around *M26* and meiotic recombination. Acetylation of histone H3 around *M26* is remarkably reduced in *gcn5*Δ, *ada2*Δ and *snf22*Δ, suggesting cooperative functions of these HAT complexes and Snf22. Conversely, Hrp1, another CHD-1 family ADCR, maintains repressive chromatin configuration at *ade6-M26*. Interestingly, transcriptional initiation site is shifted to a site around *M26* from the original initiation sites, in couple with the histone acetylation and meiotic chromatin alteration induced around 3′ region of *M26*, suggesting a collaboration between these chromatin modulators and the transcriptional machinery to form accessible chromatin. These HATs and ADCRs are also required for the regulation of transcription and chromatin structure around *M26* in response to osmotic stress. Thus, we propose that multiple chromatin modulators regulate chromatin structure reversibly and participate in the regulation of both meiotic recombination and stress-induced transcription around CRE-like sequences.

INTRODUCTION

Chromosomal DNA is compacted in chromatin structure, consisting of genomic DNA, histones, and other nonhistone proteins. The chromatin structure plays important roles in the expression and inheritance of genetic information in all eukaryotes. However, such chromatin compaction inhibits many DNA-related reactions, such as transcription, replication, DNA damage repair, and recombination, by preventing the access of transacting DNA-binding factors to the DNA substrates (Wolffe, 1997). Hence, such DNA-related reactions preferentially occur at nucleosome-free accessible chromatin regions, where the transacting factors can be easily recruited to the DNA substrates. Recent studies have revealed that posttranslational modification of histones (e.g., histone acetylation, methylation, and phosphorylation) and various chromatin remodeling complexes are required for the modulation of chromatin accessibility (Cosma *et al*., 1999; Krebs *et al*., 1999; Agalioti *et al*., 2000).

This article was published online ahead of print in *MBC in Press* (http://www.molbiolcell.org/cgi/doi/10.1091/mbc.E07–04–0377) on January 16, 2008.

Address correspondence to: Kouji Hirota (khirota@postman.riken.jp).

Homologous recombination contributes to increased genetic diversity during sexual reproduction and to proper segregation of homologous chromosomes in gametogenesis. Meiotic recombination is a highly regulated process initiated at defined chromosomal sites (recombination hotspots) that exhibit elevated levels of meiotic homologous recombination (Lichten and Goldman, 1995; Wahls, 1998; Petes, 2001; Nachman, 2002). In the yeasts *Saccharomyces cerevisiae* and *Schizosaccharomyces pombe*, it has been demonstrated that meiotic transient DNA double-strand breaks (DSBs) at these hotspots initiate a homologous recombination reaction (Sun *et al*., 1989; Steiner *et al*., 2002). It has also been demonstrated that local chromatin configuration is involved in determining the timing and position of meiotic DSB formation. For *S. cerevisiae* and *S. pombe*, chromatin around the meiotic recombination hotspot often exhibits very high sensitivity to nucleases in vitro (Ohta *et al*., 1994; Wu and Lichten, 1994; Mizuno *et al*., 1997).

The *ade6-M26* (hereafter referred as *M26*) locus in *S. pombe* is one of the most characterized meiotic recombination hotspots, which provides a good model system for studying the chromatin regulation during the activation of meiotic recombination, and even the activation of transcription coupled with the response to various extracellular stresses. The *M26* allele is a single G/T transversion in the 5′ part of the *ade6*

coding region (Ponticelli *et al*., 1988; Szankasi *et al*., 1988). This mutation creates a nonsense codon and a cAMP-responsive element (CRE)-like heptanucleotide sequence. This heptamer acts as a binding site for the transcription factor Atf1/Pcr1, which is a heterodimer of Atf1 and Pcr1 (also called Mts1/Mts2 or Gad7/Pcr1). Both the subunits are required for hotspot activation (Wahls and Smith, 1994; Kon *et al*., 1997). The *M26* mutation confers a meiosis-specific elevation of recombination of up to 20-fold, compared with control alleles, such as *ade6-M375* (*M375*) (Gutz, 1971; Ponticelli *et al*., 1988; Schuchert *et al*., 1991), which also creates an identical nonsense mutation in the codon adjacent to that generated by *M26*. We have demonstrated that the local chromatin configuration around *M26* is altered to have higher sensitivity to micrococcal nuclease (MNase) during early meiosis (Mizuno *et al*., 1997), suggesting that chromatin alteration is at least partly involved in the activation of recombination processes of *M26*. Furthermore, chromatin changes around *M26* are coupled to an altered transcription of *ade6-M26* in response to osmotic stress (Hirota *et al*., 2004). In addition, similar chromatin alteration coupled to transcriptional activation can be detected at natural *M26*-like sites that are often found in stress-responsive genes, such as *cta3*$^+$ and *fbp1*$^+$ (Hirota *et al*., 2004). Thus, chromatin alteration around *M26* and natural *M26*-like sites is also important for transcriptional regulation in response to environmental stresses.

We have further indicated that full induction of this chromatin alteration is facilitated by a histone acetyltransferase (HAT), Gcn5, and a Swi2/Snf2-like ATP-dependent chromatin remodeling factor (ADCR), Snf22, but it is repressed by the global corepressors Tup11 and Tup12 (Hirota *et al*., 2003; Yamada *et al*., 2004). Deletion of the *gcn5*$^+$ gene results in a partial loss of hotspot activity, whereas *snf22*$^+$ deletion causes a much more severe reduction (Yamada *et al*., 2004). These observations suggest that the local chromatin alteration around *M26* is vital for activation of the *M26* recombination hotspot.

There are two major classes of chromatin modifying machineries. The first class consists of covalent modifications of histone amino termini such as acetylation and methylation. In histone acetylation, a HAT complex and deacetylase complex (HDAC) add and remove acetyl groups, respectively. Increased acetylation is usually associated with derepressed chromatin configuration (Grant *et al*., 1998). HAT enzymes can be divided into several broad groups based on their conserved sequence domains. Two large families are the *S*pt-*A*da-*G*cn5 *a*cetyltransferase (SAGA) group, including Gcn5 and Ada2, and the *M*oz-*Y*bf2/*S*as3-Sas2-*T*ip60 (MYST) group (Brown *et al*., 2000; Chen *et al*., 2001). The second class of chromatin-modifying machineries consists of ADCR complexes, which alter chromatin structure by changing the location of nucleosomes by using the energy from ATP-hydrolysis (Travers, 1999). The first ADCR to be identified was the yeast Swi2/Snf2 family protein, which contains helicase/ATPase motif as a catalytic domain and a bromodomain in its C terminus. ISWI family ADCR also has a helicase/ATPase domain but lacks a C-terminal bromodomain. A further class of ADCR implicated in chromatin remodeling is the CHD family of proteins, which contains double chromodomains in its N terminus (reviewed in Travers, 1999).

Here, we investigate the functions of Mst2, a homologue of *S. cerevisiae* Sas2p or Sas3p; Ada2, a homologue of *S. cerevisiae* Ada2p; in addition to Hrp1 and Hrp3, CHD1-like ADCRs having a chromodomain, in chromatin alteration around *M26* during meiosis and stress response. We demonstrate that distinct classes of ADCRs regulate chromatin remodeling positively and negatively, giving new insight into reversible actions of chromatin remodeling at the *M26* and CRE-related sites.

MATERIALS AND METHODS

Fission Yeast Strains, Genetic Methods, and Media

The *S. pombe* strains used in this study are listed in Table 1. The genetic procedures were carried out as described by Gutz *et al*. (1974). The strains were constructed by mating haploids on a sporulation medium (SPA) (Gutz *et al*., 1974), followed by tetrad dissection. To induce meiosis using diploid *S. pombe* strains, cells were cultured in MM medium (Isshiki *et al*., 1992) supplemented with NH_4Cl as a nitrogen source to $\sim 1 \times 10^7$ cells/ml. These cells were harvested and washed with distilled H_2O (dH_2O) twice and then transferred to MM medium lacking nitrogen, to induce meiosis.

Disruption of the hrp1$^+$*, hrp3*$^+$*, ada2*$^+$*, and mst2*$^+$ *Genes*

A BLAST search using the amino acid sequences of the *S. cerevisiae* Ada2p against all translated open reading frames (ORFs) in the *S. pombe* genome enabled us to identify an SPCC24B10.08c encoding protein that exhibits strong homology to Ada2p. The ClaI-Aor51HI fragment (0.9 kb) was eliminated from the cloned *ada2*$^+$ sequence and replaced by the *ura4*$^+$ gene. The EcoRI fragment carrying *ada2::ura4*$^+$ was transformed into wild-type strain K175, and gene targeting was confirmed by polymerase chain reaction (PCR), by using an appropriate set of primers. The ORFs encoding the protein, consisting of a SWI/SNF ATPase-helicase domain and chromodomain, *hrp1*$^+$ and *hrp3*$^+$, were reported in a previous study (Yoo *et al*., 2000; Zaman *et al*., 2001). The ORF encoding Mst2 had also been reported in a previous study (Gomez *et al*., 2005). To make the strains lacking each ORF, 0.5 kbp of flanking sequence of *hrp1*$^+$, *hrp3*$^+$, and *mst2*$^+$ was cloned and ligated with the *ura4*$^+$ gene to construct *hrp1::ura4*$^+$, *hrp3::ura4*$^+$, and *mst2::ura4*$^+$, which were transformed to make the disruptants.

Determination of Recombination Rate

Each strain was grown on a yeast extract plate (YE; Moreno *et al*., 1991) supplemented with 100 mg/l adenine at 30°C. Equal volumes of each strain were mixed in 50 μl of 10 mg/ml leucine solution. Suspensions were spotted on SPA plates and incubated at 30°C for 3 d. After incubation, sporulating cells were suspended in 700 μl of 0.5% glusulase and agitated at 30°C for 30 min. After incubation, 300 μl of ethanol was added to each sample and incubated at room temperature for 5 min to kill remaining cells completely. Suspensions were centrifuged and pellets were washed with dH_2O. An appropriate number of spores was spread onto SD (Sherman *et al*., 1986) lacking adenine and YE containing adenine. Recombination rates around *M26* were calculated as follows: colony number on SD plates lacking adenine/colony number on YE plates containing adenine.

Northern Blot Analysis

Total RNA was prepared from *S. pombe* cells according to the method described previously (Elder *et al*., 1983). For the Northern blot analysis, 10 μg of total RNA was denatured with formamide, separated on 1.5% agarose gels containing formaldehyde (Sambrook *et al*., 1989), and then blotted on a charged Nylon membrane (BioDyne B membrane; Pall, East Hills, NY). The probe to detect the *ade6* transcript was prepared from a DNA fragment as described by Grimm *et al*. (1991).

Chromatin Analysis and Chromatin Immunoprecipitation

Analysis of chromatin structure by indirect end-labeling was performed according to the method of Mizuno *et al*. (1997). The DNA samples were digested with XhoI followed by Southern analysis by using the probe as described in the same study (Mizuno *et al*., 1997). Chromatin immunoprecipitation was performed according to the method of Yamada *et al*. (2004), with slight modifications as described below. Fifty milliliters of culture was incubated with 1.4 ml of 37% formaldehyde solution for 20 min at room temperature, and then 2.5 ml of 2.5 M glycine was added and incubated for 5 min. After centrifugation, collected cells were washed twice with cold Tris-buffered saline buffer (150 mM NaCl and 20 mM Tris-HCl, pH 7.5). The cells were mixed with 400 μl of lysis 500 buffer (0.1% Na-deoxycholate, 1 mM EDTA, 50 mM HEPES-KOH, pH 7.5, 500 mM NaCl, and 1% Triton X-100) for analysis in Figure 3, and 0.6 ml of zirconia beads were added. Alternatively, lysis 140 buffer (0.1% Na-deoxycholate, 1 mM EDTA, 50 mM HEPES-KOH, pH 7.5, 140 mM NaCl, and 1% Triton X-100) was used for analysis in Figure 4. After disruption of the cells using a multi-beads shocker (Yasuikikai, Osaka, Japan), the suspension was sonicated five times for 30 s each (6 times for Figure 4) to shear chromosomal DNA into ~500 base pairs fragment (DNA was sheared under 500 bp for analysis in Figure 4), and centrifuged at 4°C. The supernatant was collected as a whole-cell extract. The proper amount of antibody, in accordance with the specifications provided by the manufacturer, and 40 μl of

Table 1. *S. pombe* strains used in this study

Strain	Genotype
K26	*h*$^-$ *ade6-469 leu1-32*
K28	*h*$^+$ *ade6-M375 his5-303*
K31	*h*$^+$ *ade6-M26 his5-303*
K131	*h*$^-$ *ade6-M26 leu1-32*
K175	*h*$^+$ *ade6-M26 his5-303 ura4-D18*
K176	*h*$^-$ *ade6-M26 leu1-32 ura4-D18*
TY9	*h*$^+$ *ade6-M26 gcn5::ura4*$^+$ *uar4-D18 his5-303*
TY11	*h*$^+$ *ade6-M375 gcn5::ura4*$^+$ *uar4-D18 his5-303*
TY13	*h*$^-$ *ade6-469 gcn5::ura4*$^+$ *uar4-D18 his5-303*
PKH267	*h*$^+$ *ade6-M26 snf22::ura4*$^+$ *uar4-D18 his5-303*
PKH269	*h*$^+$ *ade6-M375 snf22::ura4*$^+$ *uar4-D18 his5-303*
PKH272	*h*$^-$ *ade6-469 snf22::ura4*$^+$ *uar4-D18 leu1-32*
PKH279	*h*$^+$ *ade6-M26 hrp1::ura4*$^+$ *uar4-D18 his5-303*
PKH281	*h*$^+$ *ade6-M375 hrp1::ura4*$^+$ *uar4-D18 his5-303*
PKH284	*h*$^-$ *ade6-469 hrp1::ura4*$^+$ *uar4-D18 leu1-32*
PKH285	*h*$^+$ *ade6-M26 hrp3::ura4*$^+$ *uar4-D18 his5-303*
PKH293	*h*$^+$ *ade6-M26 ada2::ura4*$^+$ *uar4-D18 leu1-32*
PKH296	*h*$^+$ *ade6-M375 ada2::ura4*$^+$ *uar4-D18 leu1-32*
PKH298	*h*$^-$ *ade6-469 ada2::ura4*$^+$ *uar4-D18 leu1-32*
PKH305	*h*$^-$ *ade6-469 hrp3::ura4*$^+$ *uar4-D18 leu1-32*
PKH307	*h*$^+$ *ade6-M375 hrp3::ura4*$^+$ *uar4-D18 his3-D1*
PKH314	*h*$^+$ *ade6-469 gcn5::ura4*$^+$ *ada2::ura4*$^+$ *uar4-D18 his5-303 leu1-32*
PKH316	*h*$^-$ *ade6-469 snf22::ura4*$^+$ *hrp3::ura4*$^+$ *uar4-D18 his5-303 leu1-32*
PKH318	*h*$^-$ *ade6-469 gcn5::ura4*$^+$ *hrp3::ura4*$^+$ *uar4-D18 his5-303leu1-32*
PKH322	*h*$^-$ *ade6-M26 gcn5::ura4*$^+$ *ada2::ura4*$^+$ *uar4-D18 his5-303*
PKH323	*h*$^-$ *ade6-M375 gcn5::ura4*$^+$ *ada2::ura4*$^+$ *uar4-D18 leu1-32*
PKH324	*h*$^+$ *ade6-M26 snf22::ura4*$^+$ *hrp3::ura4*$^+$ *uar4-D18 his5-303*
PKH326	*h*$^+$ *ade6-M375 snf22::ura4*$^+$ *hrp3::ura4*$^+$ *uar4-D18 his5-303*
PKH327	*h*$^+$ *ade6-M26 gcn5::ura4*$^+$ *hrp3::ura4*$^+$ *uar4-D18 his5-303*
PKH329	*h*$^+$ *ade6-M375 gcn5::ura4*$^+$ *hrp3::ura4*$^+$ *uar4-D18 his5-303*
PKH415	*h*$^-$ *ade6-M26 mst2::ura4*$^+$ *leu1-32 ura4-D18*
PKH422	*h*$^-$ *ade6-M375 mst2::ura4*$^+$ *leu1-32 ura4-D18*
PKH424	*h*$^+$ *ade6-M469 mst2::ura4*$^+$ *ura4-D18 his5-303*
PKH442	*h*$^-$ *ade6-M375 gcn5::ura4*$^+$ *mst2::ura4*$^+$ *ura4-D18*
PKH444	*h*$^+$ *ade6-469 gcn5::ura4*$^+$ *mst2::ura4*$^+$ *ura4-D18 his5-303*
PKH448	*h*$^-$ *ade6-M26 gcn5::ura4*$^+$ *mst2::ura4*$^+$ *ura4-D18 leu1-32*
D20	*h*$^+$*/h*$^-$ *ade6-M26/ade6-M26 leu1-32/+ his5-303/+*
D51	*h*$^+$*/h*$^-$ *ade6-M26/ade6-M26 hrp1::ura4*$^+$*/hrp1::ura4*$^+$ *leu1-32/+ his5-303/+ ura4-D18/ura4-D18*
D52	*h*$^+$*/h*$^-$ *ade6-M26/ade6-M26 ada2::ura4*$^+$*/ada2::ura4*$^+$ *leu1-32/+ his5-303/+ ura4-D18/ura4-D18*
D53	*h*$^+$*/h*$^-$ *ade6-M26/ade6-M26 hrp3::ura4*$^+$*/hrp3::ura4*$^+$ *leu1-32/+ his5-303/+ ura4-D18/ura4-D18*
D72	*h*$^+$*/h*$^-$ *ade6-M26/ade6-M26 mst2::ura4*$^+$*/mst2::ura4*$^+$ *leu1-32/+ his5-303/+ ura4-D18/ura4-D18*
DTY9	*h*$^+$*/h*$^-$ *ade6-M26/ade6-M26 gcn5::ura4*$^+$*/gcn5::ura4*$^+$ *leu1-32/+ his5-303/+ ura4-D18/ura4-D18*
D13A1B5	*h*$^+$*/h*$^-$ *ade6-M26/ade6-M26 snf22::ura4*$^+$*/snf22::ura4*$^+$ *leu1-32/+ his5-303/+ ura4-D18/ura4-D18*
ELD203	*h*$^+$*/h*$^-$ *ade6-M375/ade6-M375 leu3-155/+ ura1-61/+*
ELD205	*h*$^+$*/h*$^-$ *ade6-M26/ade6-M26 leu3-155/+ ura1-61/+*

DYNA-protein A beads (Dynal Biotech, Oslo, Norway) were mixed at 4°C overnight to conjugate antibody and beads, it was then washed twice with phosphate-buffered saline (PBS) (138 mM NaCl, 2.7 mM KCl, 10 mM Na_2HPO_4, and 1.8 mM KH_2PO_4) containing 0.1% BSA. Finally, 300 μl of whole-cell extract was mixed with pretreated beads and allowed to immunoprecipitate at 4°C overnight. The precipitates were washed twice with lysis 500 buffer (with lysis 140 for Figure 4), once with lysis 140 buffer, and further washed once with wash buffer (0.5% Na-deoxycholate, 1 mM EDTA, 250 mM LiCl, 0.5% NP-40, and 10 mM Tris-HCl, pH 8.0) followed by once with Tris-EDTA (TE) (10 mM Tris-HCl, pH 8.0, and 1 mM EDTA). The well-washed precipitates were mixed with 150 μl of elution buffer (10 mM EDTA, 1% SDS, and 50 mM Tris-HCl, pH 8.0) and allowed to elute the immunoprecipitated protein–DNA complexes at 65°C for 15 min (immunoprecipitation [IP] sample). The IP sample or 30 μl of whole-cell extract was mixed with 250 μl or 370 μl of 1% SDS containing TE buffer, 60 mg of proteinase K (Merck, Darmstadt, Germany) was added and incubated at 37°C for 8 h. After incubation, the temperature was shifted to 65°C, and the sample was further incubated overnight. After incubation, DNA was phenol/chloroform extracted from each of the samples and slot-blotted to a charged Nylon membrane (BioDyne B membrane; Pall), followed by Southern blot analysis to quantify DNA content. The probes were amplified from *S. pombe* genomic DNA by PCR with the following primer sets: ade6-1 (ACCAAACATCCACGGGGTCA and GTCTATTAAAAGTCGTCCAT), ade6-2 (CGTATTCTGCACTTGGTTCG and TTGTGAAATGCAACTTTAAA), ade6-3 (TGCTTGGAAATGTAACGATG and ACCTCCAAGGATCCCTACAA), ade6-4 (GGTCAATTGGGCCGAATGAT and GTGTTAATATGCTCAATTTC), and ade6-5 (TGATGCCTTGGCAGCCGTTA and TACTTTTCAGTACAAAAGGA). The probe used in Figure 3 was described in Yamada *et al*. (2004).

RESULTS

Hrp3, Ada2, and Mst2 Are Required for Full Activation of Chromatin Alteration at M26 in Meiosis, whereas Hrp1 Is Required for Its Suppression

To further understand the molecular mechanisms of chromatin alteration at *M26*, we investigated *ada2*$^+$ (a *ScADA2* homologue in *S. pombe*), *mst2*$^+$ (a homologue of *ScSAS2* and *3* in *S. pombe*), and *hrp1*$^+$, *hrp3*$^+$ (*S. pombe* CHD1-like ADCRs). We analyzed the chromatin structure around *M26* in the *ada2*Δ, *mst2*Δ, *hrp1*Δ, and *hrp3*Δ strains during the course of meiosis. The appearance of periodical MNase-cleavage patterns with ~150 base pairs at regular intervals around the *M26* site indicates that nucleosomes are positioned in the *ade6* ORF

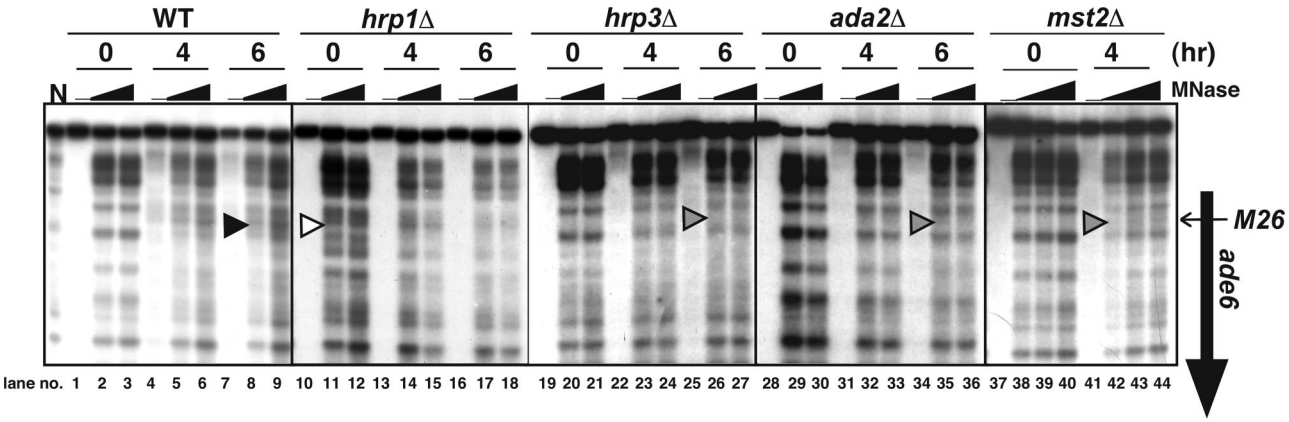

Figure 1. Hrp3 and Ada2 are required for meiotic chromatin remodeling around *ade6-M26*, whereas Hrp1 functions to suppress the alteration of chromatin structure. Diploid strains D20 (*ade6-M26*), D51 (*ade6-M26*, *hrp1*Δ), D53 (*ade6-M26*, *hrp3*Δ), D52 (*ade6-M26*, *ada2*Δ), and D72 (*ade6-M26*, *mst2*Δ) were cultured in MM + N medium (lanes 0 h). Cells were transferred to MM − N medium and cultured further for 4 h (lanes 4 h) or 6 h (lanes 6 h). Chromatin isolated from the cells was digested with MNase and analyzed as described previously (Mizuno *et al*., 1997). The vertical and horizontal arrows indicate the *ade6* ORF and position of the *M26* mutation, respectively. The arrowheads represent altered or unaltered chromatin configuration around *M26* in the wild-type (filled), *hrp1*Δ (open), *hrp3*Δ, *ada2*Δ, and *mst2*Δ (gray) strains, respectively. Lane N indicates MNase digestion of naked DNA.

under vegetative and premeiotic conditions. During meiosis, such cleavage patterns become rearranged, and an intense band occurs at the *M26* mutation site in the wild type (Figure 1, arrowhead in the wild-type lanes 5–6, 8–9). In contrast, such chromatin alteration around *M26* did not occur during meiosis in the *ada2*Δ, *mst2*Δ, and *hrp3*Δ strains as demonstrated previously in the *gcn5*Δ and *snf22*Δ strains (Yamada *et al*., 2004). Instead, a weak band occurred around *M26* meiotically (Figure 1, gray arrowheads in the *ada2*Δ, *mst2*Δ, and *hrp3*Δ, lanes 35–36, 42–44, and 26–27, respectively). Interestingly, in the *hrp1*Δ strain, MNase-cleavage patterns seemed to be like the meiotic type that exhibited an intense band at the *M26* site, even at the premeiotic time point (Figure 1, open arrowhead in *hrp1*Δ, lanes 11–12). These results suggest that Ada2, Mst2, and Hrp3 are required for the full activation of meiotic chromatin alteration at *M26*, whereas Hrp1 is required for the suppression of chromatin changes before the onset of meiosis.

Diploids of the *mst2*Δ strain could undergo meiosis, but producing abnormal asci in elevated frequency, as shown previously by Gomez *et al*. (2005). We observed meiotic progression in *ada2*Δ and *hrp3*Δ strain in the condition of synchronous meiosis by using *pat1-114* mutation (Iino and Yamamoto, 1985; McLeod and Beach, 1986), and we confirmed that *ada2*Δ and *hrp3*Δ strain, like *gcn5*Δ strain could undergo meiosis and induce meiotic DSBs formation proficiently (Supplemental Figure S1, A and B). Expression of the meiosis-specific *rec* genes *rec6*$^+$, *rec7*$^+$, *rec8*$^+$, and *rec12*$^+$ was activated, except for a slight reduction and their relative persistence in later timing (Supplemental Figure S1C). Moreover, we examined meiotic progression by monitoring meiotic nuclear divisions of nitrogen-starved diploids, and we verified that *ada2*Δ and *hrp3*Δ could undergo meiosis at kinetics similar to wild type (Supplemental Figure S1, D and E).

During the zygotic meiosis, regular asci containing four spores were efficiently formed in the *snf22*Δ mutant after a prolonged incubation (Supplemental Figure S1E), although meiotic nuclear division was seemingly defective in the *snf22*Δ (Supplemental Figure S1D). In addition, it should be noted that premeiotic DNA synthesis, meiotic DSB formation and induction of meiotic genes were only partially affected in the *snf22*Δ mutant (Supplemental Figure S1, A–C). Hence, *snf22*Δ may cause a severe delay rather than entire defects of meiotic progression. Importantly, at the same timing of early meiosis, we could not detect chromatin alteration at *M26*. This tendency was similarly observed, as we analyzed DSB formation and *M26* chromatin structure in a simultaneous meiotic culture of *pat1*$^+$ *rad50S* diploid strains (Supplemental Figure S1, F and G): little or no chromatin remodeling was observed in the *snf22*Δ mutant even at 8 h of meiotic culture, which was confirmed by the quantification of MNase sensitivity at *M26* and a control site (Supplemental Figure S1G). The ratio of sensitivity (M26/control site) meiotically increased from 0.58 to 1.39 in wild type, whereas very little change of the ratio could be detected in the *snf22*Δ (0.63 vs. 0.69). In contrast, at the same meiotic time points (8 h), genome-wide DSB formation was almost fully detectable (Figure 1). Therefore, we consider that partial defects of early meiotic events in *snf22*Δ might not be the primary reason for the loss of the *M26* chromatin remodeling in *snf22*Δ mutant. It is likely that a substantial portion of the mutant cells can undergo early meiotic events almost normally, but they cannot remodel chromatin structure specifically around *M26*, as in *gcn5*Δ (Yamada *et al*., 2004).

Effects of hrp1$^+$*, hrp3*$^+$*, ada2* $^+$*, and mst2*$^+$ *Deletion on Meiotic Recombination at M26*

The present results raise the possibility that Ada2, Mst2, Hrp1, and Hrp3 play important roles in the regulation of meiotic recombination at *M26* hotspots through chromatin modulation, because chromatin regulation has been shown to be important for the activation of recombination and transcription (Nicolas, 1998; Petes, 2001). To test this idea, we measured the recombination rates at the *ade6* locus in the *ada2*Δ, *mst2*Δ, *hrp1*Δ, and *hrp3*Δ strains by using a tester allele, *ade6-469*. The recombination rates of *M26* in the wild-type and *hrp1*Δ strains were almost indistinguishable, whereas considerable reductions in *M26* recombination rates were observed in the *ada2*Δ, *mst2*Δ, and *hrp3*Δ strains (Figure 2A). The recombination rates of the control allele, *M375*, which does not exhibit hotspot activity, were not affected significantly in the *ada2*Δ, *hrp1*Δ, and *hrp3*Δ strains, whereas

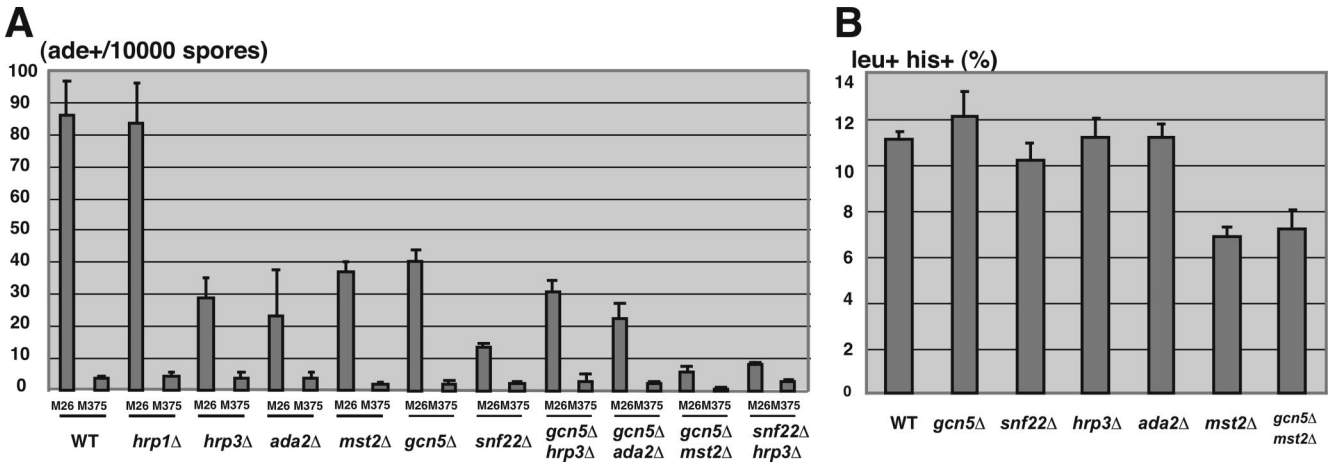

Figure 2. The impact of *hrp1*$^+$, *hrp3*$^+$, *ada2*$^+$, and *mst2*$^+$ deletions on meiotic recombination frequency and meiotic DSB formation and genetic interactions between these proteins and Gcn5 or Snf22. (A) Recombination rates at *M26* or *M375* control allele (indicated as Ade$^+$/10^4 spores) were examined as described in *Materials and Methods*. All crosses were repeated independently at least three times. Error bars represent SD. (B) Recombination between *leu1-32* and *his5-303* (indicated as leu+/his+ [percentage]) was measured as described in *Materials and Methods*. All crosses were repeated independently two or three times. Error bars represent SD.

a more severe reduction was observed in the *mst2*Δ strain (WT, 3.6 ± 0.6 ade$^+$/10^4 spores, n = 7; *mst2*Δ, 1.6 ± 0.26 ade$^+$/10^4 spores, n = 3 [~2.3-fold reduction]; Figure 2A). The recombination frequency in *M26* and *M375* was reduced by almost the same degree in the *mst2*Δ strain (WT, 86.1 ± 10.6 ade$^+$/10^4 spores, n = 7; *mst2*Δ, 36.7 ± 2.5 ade$^+$/10^4 spores, n = 3 [~2.3-fold reduction]; Figure 2A). These results suggest that Ada2 and Hrp3 are required for the activation of meiotic recombination in an *M26* hotspot-dependent manner, as demonstrated previously in the *gcn5*Δ and *snf22*Δ strains (Yamada *et al*., 2004). These also suggest that Mst2 is involved in the global recombination.

We also examined the recombination rates between *leu1* and *his5* loci (intergenic recombination) in *hrp1*Δ, *hrp3*Δ, *ada2*Δ, and *mst2*Δ strains. A less severe but significant reduction was observed only in the *mst2*Δ strain, consistent with its severe defects in recombination frequency observed in *M375* control allele (WT, 11.1 ± 0.35%, n = 2; *mst2*Δ, 6.9 ± 0.42%, n = 2 [~1.6-fold reduction]; Figure 2B). More importantly, the recombination rates between *leu1-32* and *his5-303* in *ada2*Δ, *hrp1*Δ, and *hrp3*Δ strains were very similar to those observed in the wild-type strain (Figure 2B). Taken together, we concluded that the *ada2*Δ and *hrp3*Δ mutant effects, like the *snf22*Δ and *gcn5*Δ effects, are specific for the recombination at the *M26* hotspot.

We further tested genetic interactions between *ada2*Δ or *mst2*Δ or *hrp3*Δ and *gcn5*Δ (or *snf22*Δ) mutations. The cells lacking *gcn5*$^+$ showed a partial reduction in recombination rate (~50%, Figure 2A; Yamada *et al*., 2004). However, the double deletions of the *gcn5*$^+$ and *ada2*$^+$ or *hrp3*$^+$ genes did not show a further decrease in *M26* recombination frequency, indicating that both Ada2 and Hrp3 function along the same pathway as Gcn5 (Figure 2A). Interestingly, the double deletions of the *gcn5*$^+$ and *mst2*$^+$ resulted in drastic reduction of recombination frequency in *M26*, indicating that Mst2 and Gcn5 participate in distinct pathways (Figure 2A). Furthermore, a *snf22*$^+$ deleted strain showed a severe reduction in *M26* recombination frequency (Figure 2A; Yamada *et al*., 2004). The *ada2*Δ/*snf22*Δ double-deleted strain exhibited a completely sterile phenotype; hence, we could not analyze the recombination rate in this strain. The deletion of the *hrp3*$^+$ gene in addition to the *snf22*$^+$ deletion showed slight or little reduction in the recombination rate at *M26* (Figure 2A). This result suggests that Hrp3 and Snf22 generally function along the same pathway, but it is also possible that Hrp3 has some roles partly distinct from Snf22.

The Level of Histone H3 Acetylation around M26 Is Decreased in snf22Δ, gcn5Δ, and ada2Δ

Hyperacetylation of histone H3 or H4 is often found in transcriptionally and recombinationally active chromosomal domains, such as transcription active loci and the gene conversion active chicken immunoglobulin locus (Brown *et al*., 2000; Seo *et al*., 2005). Hyperacetylation of histones is also observed around *M26* during early meiosis. It requires the *M26* sequence, its binding protein Atf1 and the Gcn5 HAT (Yamada *et al*., 2004). Thus, we investigated and compared the acetylation levels of histones H3 and H4 in the *snf22*Δ, *gcn5*Δ, *hrp1*Δ, *hrp3*Δ, *ada2*Δ, and *mst2*Δ strains. To examine the acetylation level of histones, we used chromatin immunoprecipitation (ChIP) analysis by using anti-acetylated histone H3 or H4, as described previously (Yamada *et al*., 2004). The DNA from the immunoprecipitated and input materials were transferred to slot blots and hybridized with a sequence of the *ade6* locus (around the *M26* hotspot as shown in Figure 4A) (Figure 3A). The acetylation levels of histone H3 and H4 around *M26* were elevated at 0.5–1 h after nitrogen starvation in the wild-type cells. In the *gcn5*Δ, *ada2*Δ, and *snf22*Δ strains, however, histone H3 acetylation levels around *M26* were not as significantly increased, and the histone H3 acetylation stayed at very low levels (Figure 3B). A less severe decrease in histone H4 acetylation was observed in the *gcn5*Δ and *ada2*Δ strains (Figure 3B). In contrast, the acetylation level of histone H4 is decreased in *snf22*Δ, suggesting that Snf22 plays some role in facilitating the acetylation of histones H3 and H4. Importantly, little increase in histone H3 acetylation was observed in the *hrp3*Δ strain (Figure 3B), which is consistent with its effects on recombination rate at *M26* (Figure 2A). Moreover, the basal level of histone H3 acetylation in *hrp1*Δ, which had constitutively an open chromatin configuration around *M26* (Figure 1), was significantly higher (~1.5-fold) than wild-type levels. Furthermore, it should be noted that no decrease in the acetylation of histones H3 and H4 was observed in the *mst2*Δ strain (Figure 3B).

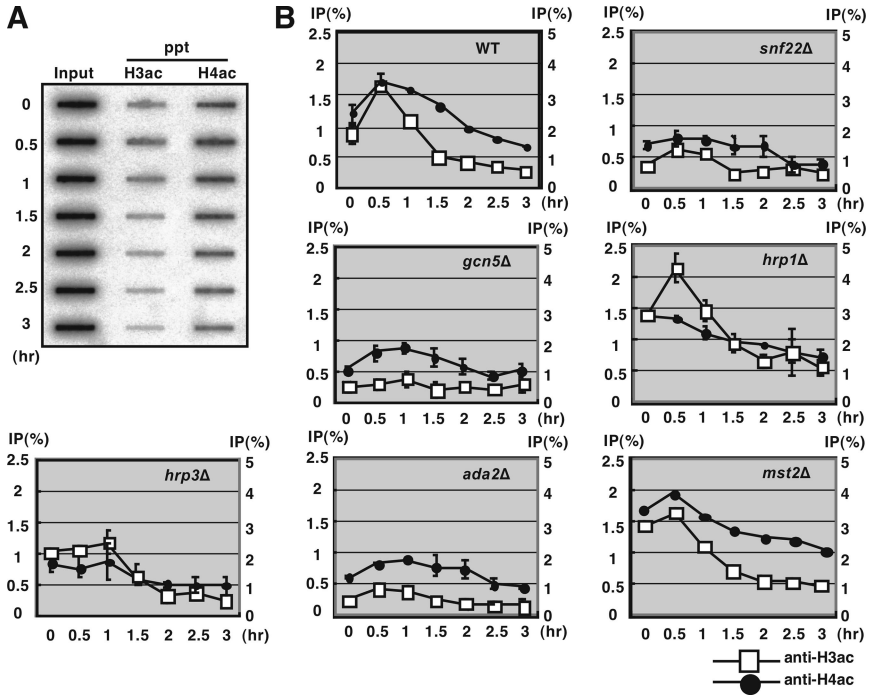

Figure 3. Hyperacetylation of histone H3 around the *M26* mutation site was affected in the *gcn5*Δ, *snf22*Δ, and *ada2*Δ strains. (A) The diploid wild-type strain was cultured to induce meiosis, as described in Figure 1. DNA of the input and ChIP samples were quantified by a slot blotting followed by hybridization with the *M26* probe. The time after meiotic induction is indicated on the left side of the panel. (B) Quantified data of acetylated histones H3 and H4 in wild-type, *gcn5*Δ, *snf22*Δ, *hrp1*Δ, *hrp3*Δ, *ada2*Δ, and *mst2*Δ strains. Vertical and horizontal axes represent ChIP efficiency (percentage) (left, histone H3ac; right, histone H4ac) and hours after meiotic induction. Squares and filled circles indicate data for acetylated histones H3 and H4, respectively. All experiments except for *mst2*Δ were repeated independently two times. Error bars represent SD.

M26 Mediates Site-specific Acetylation of Histones H3 and H4 and Transcriptional Activation

The acetylation of histone H3 around *M26* occurs in early meiosis, in which Gcn5-Ada2 and Snf22 are required (Figure 3B). However, the relation of histone acetylation and ATF/CREB transcription factor, Atf1, binding on *M26* has not been fully elucidated. To address this issue, we investigated histone acetylation in the course of meiosis in *M26* and *M375* diploids more precisely. As illustrated in Figure 4A, for the quantitative analysis, the *ade6* locus around the *M26* or *M375* site was divided into fragments of 200 base pairs, and the probes for each region were used to measure ChIP efficiency at those segments. To view the difference in acetylation level at high resolution, ChIP procedure was modified, as described in *Materials and Methods*. We found that the acetylation of histones H3 and H4 around *ade6* promoter (probes 1, 2, and 3) was observed in the both *M26* and *M375* strains in early meiosis. Interestingly, strong acetylation of histone H3 was detected only in the *M26* strain at the 3′ region of the *M26* mutation site (*M26/M375*, >2.5-fold; Figure 4B). The acetylation of histone H4 was also observed in this region (probes 4 and 5) in the *M26* strain rather than in *M375*, whereas the effect of *M26* mutation was lower than that of histone H3 acetylation (*M26/M375*, <1.4-fold; Figure 4B). Consistent with this observation, the chromatin remodeling was observed around 3′ region of *M26* mutation point in meiosis (Figure 4C).

Hyperacetylation of histones H3 and H4 and chromatin remodeling are assumed to be related to transcriptional activation. We investigated the transcript of the *ade6* gene in the course of meiosis by Northern analysis. As shown in Figure 4D, a shorter version of the *ade6* transcript was observed in the *M26* strain; however, this short transcript was not seen in the *M375* strain. Furthermore, the amount of the short transcript in the *M26* strain was elevated in the course of meiosis (Figure 4E). To examine whether the short version of the *ade6* transcript was initiated from 3′ region of the original initiation site, we hybridized probe 3 in Figure 4A on the same membrane. As shown in Figure 4D, only a long version of the *ade6* transcript was detected by probe 3, indicating that the transcriptional initiation site was shifted from the original initiation site to the 3′ region of probe 3 in the short version of the transcript. Moreover, we determined the initiation site of the shorter transcript observed in *ade6-M26* by rapid amplification of cDNA ends (RACE) analysis, as described in the Supplemental Material. Interestingly, the shorter transcript was initiated from 2 base pairs upstream of the *M26* heptanucleotide sequence (Supplemental Figure S2). These results indicate that Atf1 binding on *M26* provokes site-specific hyperacetylation of histones and the initiation of transcription followed by activation of recombination.

Furthermore, we examined whether the HATs and ADCRs required for the recombination in *M26* are involved in the shift of the transcription initiation site of *ade6* during meiosis. As shown in Figure 4F, the shorter *ade6* transcript was detected in the diploid *snf22*Δ, *gcn5*Δ, *hrp3*Δ, and *ada2*Δ strain as in a diploid wild-type strain before meiosis, but the intensity of the shorter transcript did not increase in these mutants during meiosis (Figure 4F). These results indicate that these HATs and ADCRs are not required for the shift per se, whereas the transcriptional activation of shorter RNA is dependent on these HATs and ADCRs.

Cells Lacking hrp3$^+$ or ada2$^+$ Cannot Induce Chromatin Alteration at M26 in Response to Osmotic Stress

We previously demonstrated that chromatin alteration and transcriptional activation in *ade6-M26* are induced in response to osmotic stress (Hirota *et al*., 2004). Therefore, we next examined the effects of deleting the *snf22*$^+$, *gcn5*$^+$, *ada2*$^+$, *hrp1*$^+$, and *hrp3*$^+$ genes on chromatin structure around *M26* under osmotic stress using haploid cells. In wild-type cells, we detected changes in MNase-sensitive band patterns. An intense band occurred at the *M26* mutation site when cells were exposed to 1.2 M of sorbitol (Figure 5C, filled arrowhead, lanes 5, 6). Under such conditions, the

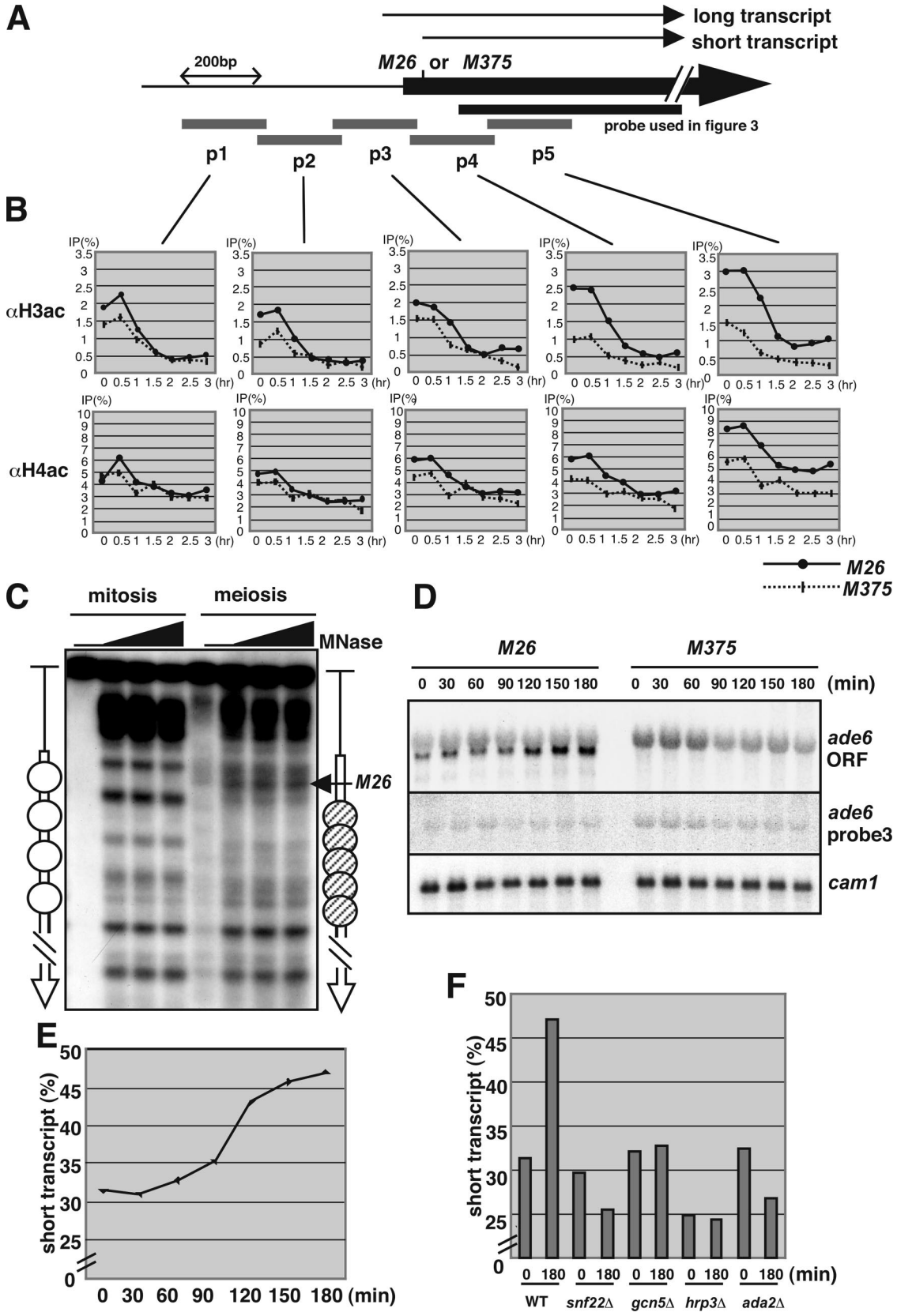

Figure 4. *M26* specific hyperacetylation of histones H3 and H4, and transcriptional activation. (A) Schematics of the probes used to quantify the acetylation of histones H3 and H4 around the *ade6* locus. The scale represents 200 bp. Arrows represent the initiation sites of long and short transcript. (B) Quantified data for acetylated histones H3 and H4 in *M26* (bold line) and *M375* (dotted line) strains. Vertical and horizontal axes represent ChIP efficiency (percentage) and hours after meiotic induction. (C) Meiotic chromatin remodeling is induced around 3′ region of

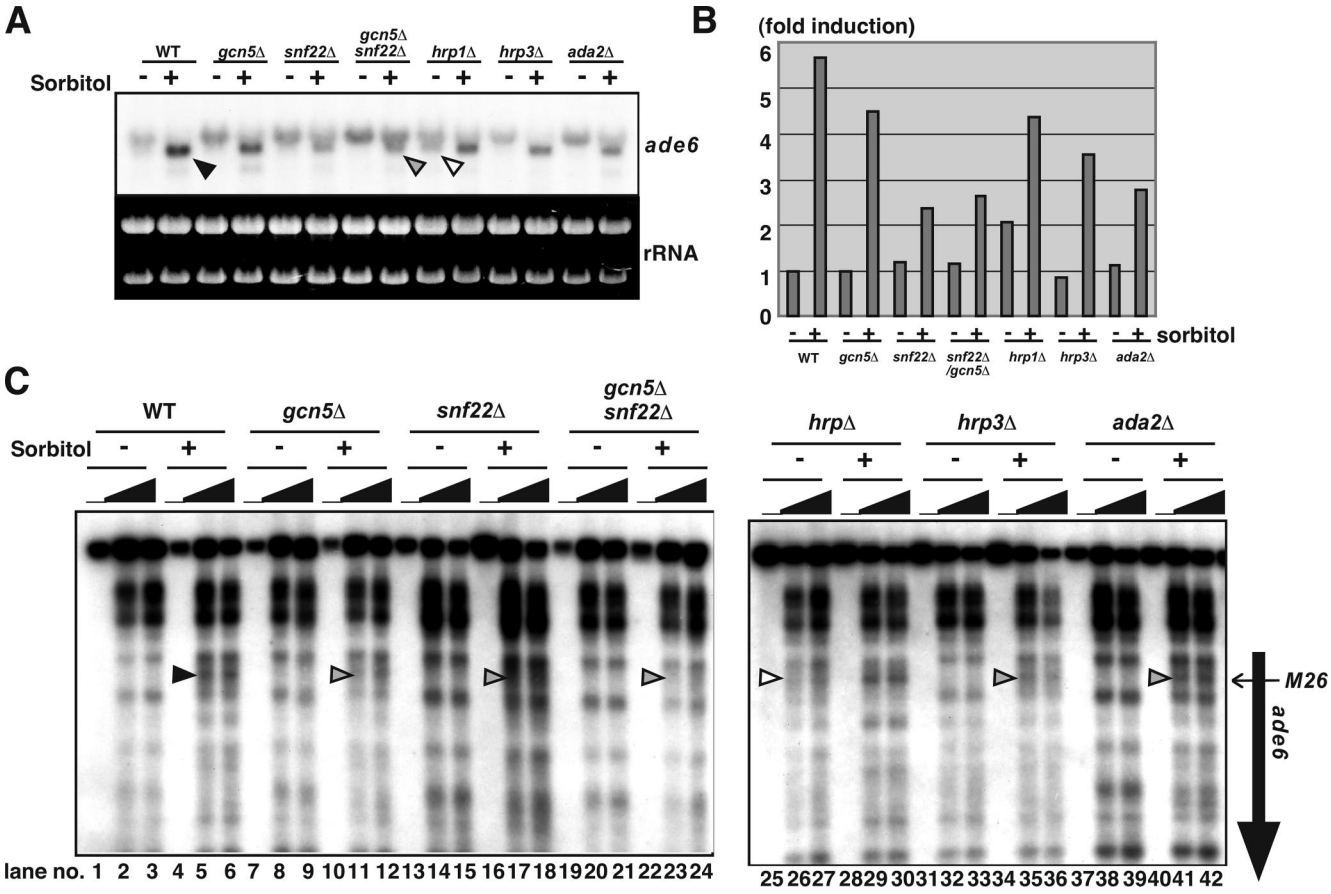

Figure 5. The chromatin regulation of *ade6-M26* by the HATs and ADCRs is coupled to transcriptional activation in response to osmotic stress. (A) The cells of haploid strains (wild type, *gcn5*Δ, *snf22*Δ, *gcn5*Δ/*snf22*Δ, *hrp1*Δ, *hrp3*Δ, and *ada2*Δ) were cultured in YE to mid-log phase, transferred to YE containing 1.2 M sorbitol, and cultured further for 90 min. Total RNA was isolated from each culture and analyzed by Northern analysis. Arrowheads represent the shorter *ade6-M26* transcript. (B) Quantification of the results in A. Vertical axis indicates -fold induction compared with the mRNA levels in the wild-type strain without the sorbitol treatment. (C) The crude nuclei were isolated from the simultaneous cultures indicated in Figure 5A. The chromatin structure was analyzed as described in Figure 1. The vertical and horizontal arrows indicate the *ade6* ORF and position of the *M26* mutation, respectively. Arrowheads represent the altered or partially altered chromatin configuration around *M26* in the wild-type (filled), *hrp1*Δ (open), *hrp3*Δ, *ada2*Δ, and *mst2*Δ (gray) strains, respectively.

size and amount of the *ade6* transcripts became smaller and more abundant (~sixfold increase; Figure 5A, filled arrowhead). In addition, we determined the initiation site of smaller RNA observed when cells were exposed to sorbitol (osmotic) stress by RACE analysis (data not shown). The shorter transcript was initiated from 48 base pairs downstream of *M26* heptanucleotide sequence, indicating smaller RNA induced by osmotic stress is initiated from a close but distinct site from that of shorter meiotic RNA shown in Figure 4.

In the *gcn5*Δ, *snf22*Δ, *ada2*Δ, and *hrp3*Δ strains, alterations in chromatin structure at the *ade6-M26* locus were reduced (Figure 5C, gray arrowhead, lanes 11–12, 17–18, 41–42, and 35–36, respectively). It should be noted that the impact of these mutations upon transcription in *ade6-M26* (the shorter transcript, 1.3~2.0-fold reduction compared with wild type) was much smaller than their effects on meiotic recombination at *M26* (2.5~10-fold reduction compared with wild type). Conversely, in the *hrp1*Δ strain, chromatin configuration around *M26* was constitutively open to some extent, even without the treatment of sorbitol (Figure 5C, open arrowhead, lanes 26 and 27). In addition, consistent with the constitutive openness of the chromatin configuration at *M26*, a twofold induction of the short version of the *ade6-M26* transcript was observed even in the absence of sorbitol (Figure 5, A and B, open arrowhead). Interestingly, the magnitude of the transcriptional induction was reduced in the *hrp1*Δ strain (sorbitol+/sorbitol−; WT ~sixfold, *hrp1*Δ ~twofold, Figure 5B), indicating that proper regulation of

Figure 4 (cont). *M26* mutation point. Wild-type (D20) cells were cultured in MM + N (lanes; mitosis) and transferred to MM − N and cultured further for 4 h (lanes; meiosis). Open and hatched ovals represent phase and randomly positioned nucleosomes, respectively. (D) The initiation site of the *ade6* transcript is shifted to the 3′ region in the *M26* strain. The diploid *M26* and *M375* strains were cultured to induce meiosis, as described in Figure 1. RNA was isolated and analyzed by Northern blotting using the ade6-ORF probe, probe 3 in Figure 4A, and *cam1*$^+$ as a loading control (Takeda and Yamamoto, 1987). (E) The intensity of the band corresponding to the short transcript and whole transcript was quantified, and relative band intensity (short transcript/whole transcript percentage) was calculated. (F) The increase of short transcript of *ade6* during meiosis requires Snf22, Gcn5, Hrp3, and Ada2. The diploid wild-type, *snf22*Δ, *gcn5*Δ, *hrp3*Δ, and *ada2*Δ strains were cultured to induce meiosis, as described in Figure 1, and transcript of *ade6* was detected as Figure 4D. The relative intensity (short transcript/whole transcript percentage) was calculated as Figure 4E.

the chromatin structure is vital for effective induction of transcription. All mutants of *snf22*Δ, *gcn5*Δ, *ada2*Δ, *hrp1*Δ, and *hrp3*Δ conferred severe defects in chromatin alteration and transcriptional phase transition in *ade6-M26* when cells were exposed to osmotic stress (Figure 5).

These results led us to speculate that these genes might be involved in cellular responses to other environmental stresses. As shown in Supplemental Figure S3, deletion of *snf22*Δ, *gcn5*Δ, *ada2*Δ, *hrp1*Δ, and *hrp3*Δ results in various stress-sensitive phenotypes. For example, the *snf22*Δ, *hrp1*Δ, and *hrp3*Δ strains were all severely and weakly sensitive to cation (1 M KCl) and glucose starvation stresses, respectively (Supplemental Figure S3). Interestingly, these mutants showed little sensitivity to osmotic stress (1.2 M sorbitol). In addition, replication stress hydroxyurea (HU)-sensitive phenotypes were observed in the *snf22*Δ, *gcn5*Δ, *hrp1*Δ, and *ada2*Δ strains. Furthermore, the *ada2*Δ and *gcn5*Δ mutants exhibited weak sensitivity to UV and methylmethane sulfonate (Supplemental Figure S3).

To address the reasons for the partial sterility of *snf22*Δ and complete sterility of the *snf22*Δ/*ada2*Δ double mutant, we examined their ability to cause G1 phase arrest in response to nitrogen starvation. This is because the G1 phase serves as an exit for cell differentiation, such as mating and meiotic induction processes (Yamamoto *et al*., 1997). Wild type and *ada2*Δ cells could accumulate in the 1C population in response to nitrogen starvation, indicating that these strains can arrest the cell cycle in G1 phase (Supplemental Figure S4). In contrast, *snf22*Δ cells exhibited only partial accumulation at 1C, indicating that *snf22*Δ has a defect in G1 phase arrest in response to nitrogen starvation. Furthermore, this defect of *snf22*Δ in cell-cycle arrest was strengthened in the *snf22*Δ/*ada2*Δ double mutant (Supplemental Figure S4). Alternatively, it is also possible that Snf22 and Ada2 is involved in the induction of some genes required for mating, because a significant amount of cells arrested in G1 phase in *snf22*Δ/*ada2*Δ double mutant, whereas this mutant shows complete sterile phenotype.

These results suggest that Snf22, Gcn5, Hrp1, Hrp3, and Ada2 are pivotal for appropriate cellular response to various environmental stresses, possibly via chromatin regulation, as shown in *ade6-M26*.

DISCUSSION

This study on fission yeast, demonstrates the in vivo function of Ada2 (a putative *S. pombe* SAGA component), Mst2 (a MYST family HAT), and Hrp1, Hrp3 (ADCRs having a chromodomain) in chromatin remodeling processes at *M26*, which provides a good model system for studying chromatin regulation around CRE-related *cis*-acting DNA sequences. Ada2, Hrp1, and Hrp3 play essential roles in chromatin remodeling, activation of meiotic recombination, and transcriptional response to osmotic stress at *M26*. Additionally, Mst2 is involved in global recombination possibly via the chromatin remodeling process. Moreover, Hrp1, Hrp3, and Snf22—three distinct entities of ADCR—have redundant and antagonizing functions in regulating chromatin alteration at *M26*; Hrp3 and Snf22 function to form an open chromatin configuration, whereas Hrp1 plays a suppressive role.

HAT and ADCR Components Function Together in Chromatin Modification and Recombination Activation at M26

These results indicate that chromatin alteration at *M26* is controlled by multiple chromatin modulators. Both Ada2 and Gcn5 are shown to be equally needed for hyperacetylation of histone H3 around *M26*, and for meiotic recombination enhancement and chromatin changes around *M26* (Figures 1–3). In addition, the *ada2*Δ/*gcn5*Δ double deletion confers defects in *M26* recombination hotspot activation during meiosis at comparable levels to the *ada2*Δ mutants. This result, together with the cooperative action of their *S. cerevisiae* counterparts in the SAGA complex in specific transcriptional responses (Grant *et al*., 1998), suggests that they function in concert in a SAGA-like complex to regulate chromatin configuration and recombination competency at *M26*.

Interestingly, Mst2 is required for efficient recombination in the *ade6* locus (both of *M26* and *M375*) but not for acetylation of histones H3 and H4. This suggests its involvement possibly in the formation of stable remodeling complexes, besides its function as a HAT in the recombination. The recombination frequency in the *leu1–his5* interval is less severely affected than in the *ade6* locus of the *mst2*Δ mutant. It has previously been shown that recombination frequency in the *his4–lys4* interval is not decreased in the *mst2*Δ strain (Gomez *et al*., 2005). This suggests that the impact of the lack of Mst2 on recombination depends on the locus observed, possibly because of the context of the local chromatin structure.

Gcn5 and Snf22 are both required for the complete chromatin changes around *M26*. We previously demonstrated that the double deletion of $snf22^+$ and $gcn5^+$ genes results in *snf22*Δ like defects in chromatin remodeling and meiotic recombination enhancement at *M26* (Yamada *et al*., 2004). We thus hypothesized that Snf22 ADCR and Gcn5 HAT play roles in the same pathway, and that Gcn5 HAT may function at earlier stages than Snf22 to facilitate the specific entry of ADCR to the *M26* sites. However, unexpectedly, the Gcn5-dependent hyperacetylation of histone H3 around *M26* is highly dependent on Snf22 (Figure 3), suggesting that they may act in an interdependent manner. This can be explained by the idea that Snf22 facilitates Gcn5 entry to the *M26* site by forming a HAT-ADCR loading complex (Figure 6A).

Given the interdependent relation between Gcn5 and Snf22, the next question is why the *gcn5*Δ single mutant has only partial defects in meiotic chromatin alteration and recombination activation at *M26*. In addition, deletion of Ada2 or Gcn5 HAT cause only partial reduction in *M26*-dependent hyperacetylation of histone H4 (Figure 3; Yamada *et al*., 2004). Most simply, in comparison with Gcn5 HAT, Snf22 has a more general role in loading of SAGA and NuA4 HAT complexes, presumably via recruitment of Tra1-like protein containing HAT complexes (Allard *et al*., 1999). This notion is consistent with the observation that the acetylation of histone H4 severely decreases in *snf22*Δ. Alternative rationale is that other types of HATs are responsible for the hyperacetylation of histone H4 and function redundantly in chromatin modulation with Ada2 and Gcn5, which are mainly involved in H3 hyperacetylation. In the budding yeast, *nu*cleosomal *a*cetyltransferase of histone H4 (NuA4), a multiprotein HAT complex that preferentially acetylates histone H4, has been purified and shown to contain the MYST-family HAT Esa1 as the catalytic subunit (Allard *et al*., 1999). The fission yeast *ESA1* homologue $mst1^+$ is cloned, and it was shown to be essential for viability (Gomez *et al*., 2005). Therefore, for the investigation of the genetic relation between $mst1^+$ and $gcn5^+$ (or $ada2^+$) HAT, we need to newly isolate conditional mutants of $mst1^+$ in the future work.

The Reversible Control Mechanism for Chromatin Remodeling

Many ADCRs, such as ISWI and SWI/SNF, are assumed to primarily increase DNA accessibility in chromatin by disrupting local nucleosomal arrays (reviewed in Travers,

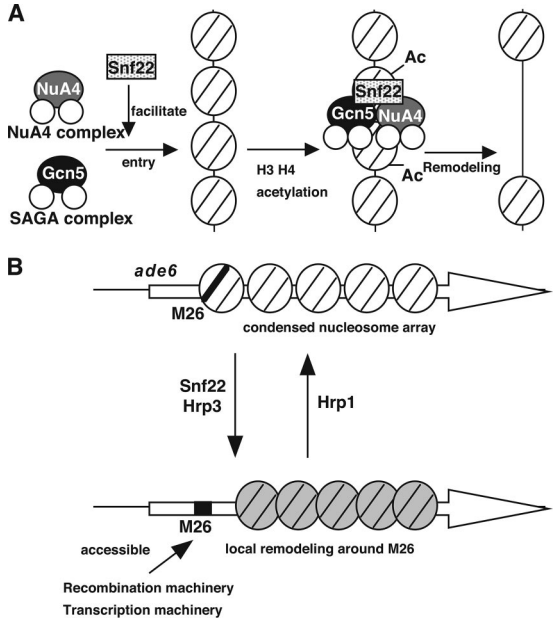

Figure 6. (A) Cooperative behavior of HATs-ADCRs for the modification and remodeling of chromatin structure around *M26*. (B) Reversible regulation of *M26*/CRE-dependent chromatin remodeling by chromatin modifying machineries. The model postulates that distinct remodeling complexes are required for nucleosome disruption to recruit either recombination complexes or transcription complexes. In addition, Hrp1 is involved in the suppression of chromatin remodeling at *M26*, thereby providing reversible regulation of the *M26*/CRE-dependent chromatin configuration.

1999). However, the present data demonstrate that one of the CHD-1 like ADCRs, Hrp1, plays a role in suppressing chromatin opening, whereas Snf22 and Hrp3 ADCRs act to establish an open chromatin configuration at *M26*. This indicates that chromatin regulation by ADCRs is reversible and that the status of local chromatin structure is controlled by dynamic shifts of equilibrium between inverse reactions by distinct types of ADCRs (Figure 6B). This is supported by previous reports that human Mi2, a chromodomain ADCR, has been copurified with HDAC1 and 2 in the NuRD complex (Tong *et al*., 1998; Zhang *et al*., 1998), which seem to form a repressive (inaccessible) chromatin configuration. An alternative but nonexclusive possibility is that Hrp1 represses Snf22 and Gcn5-dependent chromatin remodeling under certain conditions, such as during vegetative growth. Our preliminary experiments indicate that double or triple mutants of *hrp1*Δ/*snf22*Δ, *hrp1*Δ/*gcn5*Δ, and *hrp1*Δ/*gcn5*Δ/*snf22*Δ confer defects in meiotic chromatin alteration at *M26*, suggesting that Gcn5 and Snf22 are essential in the Hrp1-dependent constitutive disclosure of chromosomal DNA at *M26* (Mizuno, unpublished observation).

CREB/ATF-M26 Complex Provides Hyperacetylation of Histone H3 Followed by Initiation of Transcription and Recombination

The acetylation of histones H3 and H4 is enriched at the 3′ region of the *M26* mutation site, whereas such hyperacetylation was not observed in the *M375* control allele that lacks the binding site for Atf1 (Figure 4). The acetylation of histones H3 and H4 also occurs in the promoter region of the *ade6* gene in both *M26* and *M375* alleles, indicating that site-specific hyperacetylation is provided by Atf1 binding on *M26*, and is pivotal for specific activation of recombination. Gcn5-Ada2 HAT and Snf22 is required for this hyperacetylation. These results suggest Atf1 recruits Gcn5-Ada2 HAT and Snf22 to acetylate histone in the targeted region. However, in the present ChIP condition, we cannot detect the binding of Gcn5 to *M26* in the course of meiosis, which may be due to a transient interaction of Gcn5 to *M26*.

Interestingly, *M26* strain produces a smaller transcript that is initiated from 2 base pairs upstream of the *M26* site. In addition, the smaller transcript exists before induction of meiosis and increases during the course of meiosis, indicating that transcriptional initiation site is shifted to *M26* and the transcription of shorter RNA is activated during meiosis (Figure 4, D and E). Furthermore, the HATs and ADCRs required for the recombination at *M26* is also essential for the meiotic transcriptional activation of shorter RNA, but they are not required for the shift of initiation site before meiosis per se (Figure 4F). *M26* dependent hyperacetylation of histone H3 and H4 and chromatin remodeling was observed at 3′ region of *M26* site (Figure 4, B and C), implicating a possible role of RNA polymerase II (RNAPII) in chromatin remodeling process. In addition, the HATs and ADCRs were required for the hyperacetylation of histones and elevation of smaller transcript in meiosis. Thus, we speculate the possible model that RNAPII may function to induce chromatin remodeling at 3′ region o *M26* site collaborating with the HATs and ADCRs during meiosis to gain access of proteins required for DSB formation. This model explains the reason why histone acetylation occurred in earlier stage before DSB formation. This model is also supported by previous studies; Orphanides and Reinberg had suggested that RNAPII elongates through the transcribed region with disrupting chromatin, cooperatively with HAT and other remodeling complexes (Orphanides and Reinberg, 2000). In addition, it had been reported the PCAF (HAT complex) binds specifically to the phosphorylated, elongating form of RNAPII (Cho *et al*., 1998). Further investigation might be necessary to clarify the role of RNAPII in chromatin regulation in *M26*.

Roles of CRE-dependent Chromatin Modifiers in Transcriptional Regulation

Conversely, it is obvious that the initiation site of *ade6* transcript is also shifted under osmotic stress (Figure 5). It is important that the HATs and ADCRs reported here are also involved in the shift of the initiation site and transcriptional activation of *ade6-M26* in response to osmotic stress (Figure 5). Indeed, the initiation site of the shorter transcript under osmotic stress is not identical, but very close to that of meiotic short RNA. This suggests that *M26* transcriptions in meiosis and osmotic stress are regulated by generally common but slightly different mechanisms. In addition, the same HATs and ADCRs function in both mechanisms. Possibly, the regulation of chromatin structure by the HATs and ADCRs is pivotal to both osmotic response (the shift of the initiation site of *ade6*) and meiotic recombination activation at *M26*. Moreover, they may be required for proper adaptation against various environmental stresses, presumably by proper induction of appropriate genes via modulating the local chromatin configuration (Supplemental Figure S3). Alternatively, it is also possible that histone acetylation is pivotal for DNA repair process via chromatin regulation, because *ada2*Δ and *gcn5*Δ mutants exhibited DNA damage sensitive phenotype. The present result together with previous finding in *S. cerevisiae* support this possibility (Bird *et al*., 2002; Downs *et al*., 2004; van Attikum *et al*., 2004). Hence, these *M26*-dependent (in other words, CRE-dependent)

chromatin modifiers have multiple roles in site-specific recombination activation and stress-induced transcriptional activation at *M26* or CRE-related *cis*-acting DNA sequences. Because shortening of the *ade6-M26* transcript is at least partly coupled with transcriptional activation and chromatin alteration around *M26*, those HATs and ADCRs are involved in the access of RNAPII or basic transcription factors at the level of chromatin structure. Recently, it has also been shown that CHD remodelers (Hrp1 and Hrp3) interacting with Nap1 histone chaperone participate in nucleosome disassembly at promoters, suggesting possible roles of these remodelers in the transcriptional regulation via chromatin modulation (Walfridsson *et al*., 2007). The combination of Tup1-like global corepressors, and some sequence-specific coregulators, such as Rst2 and Scr1 Zn-finger protein, probably governs the differential responses of chromatin structure in response to distinct stresses (Hirota *et al*., 2003; Hirota *et al*., 2004; Hirota *et al*., 2006).

The study suggests the redundant and antagonistic roles of these HATs and ADCRs in chromatin remodeling. These factors might play pivotal roles in regulating chromatin dynamics in the cellular response to environmental stresses. Further understanding of those factors might shed light on this essential mechanism of regulation.

ACKNOWLEDGMENTS

K.H. thanks all members of the Genetic System Regulation Laboratory and Cellular and Molecular Biology Laboratory in RIKEN for helpful discussions and T. Yamada for critical advice on ChIP analysis. We thank K. Yamada for critical reading of this manuscript. We also thank Y. Ichikawa and R. Nakazawa for DNA sequencing and Y. Sakuma for technical assistance. This work was supported by grants from the following sources: basic research from the Bio-oriented Technology Research Advancement Institution (to T.S. and K.O.); grants-in-aid for scientific research on priority areas from the Ministry of Education, Science, Culture and Sports, Japan (to K.O.).

REFERENCES

Agalioti, T., Lomvardas, S., Parekh, B., Yie, J., Maniatis, T., and Thanos, D. (2000). Ordered recruitment of chromatin modifying and general transcription factors to the IFN-beta promoter. Cell *103*, 667–678.

Allard, S., Utley, R. T., Savard, J., Clarke, A., Grant, P., Brandl, C. J., Pillus, L., Workman, J. L., and Cote, J. (1999). NuA4, an essential transcription adaptor/histone H4 acetyltransferase complex containing Esa1p and the ATM-related cofactor Tra1p. EMBO J. *18*, 5108–5119.

Bird, A. W., Yu, D. Y., Pray-Grant, M. G., Qiu, Q., Harmon, K. E., Megee, P. C., Grant, P. A., Smith, M. M., and Christman, M. F. (2002). Acetylation of histone H4 by Esa1 is required for DNA double-strand break repair. Nature *419*, 411–415.

Brown, C. E., Lechner, T., Howe, L., and Workman, J. L. (2000). The many HATs of transcription coactivators. Trends Biochem. Sci. *25*, 15–19.

Chen, H., Tini, M., and Evans, R. M. (2001). HATs on and beyond chromatin. Curr. Opin. Cell Biol. *13*, 218–224.

Cho, H., Orphanides, G., Sun, X., Yang, X. J., Ogryzko, V., Lees, E., Nakatani, Y., and Reinberg, D. (1998). A human RNA polymerase II complex containing factors that modify chromatin structure. Mol. Cell. Biol. *18*, 5355–5363.

Cosma, M. P., Tanaka, T., and Nasmyth, K. (1999). Ordered recruitment of transcription and chromatin remodeling factors to a cell cycle- and developmentally regulated promoter. Cell *97*, 299–311.

Downs, J. A., Allard, S., Jobin-Robitaille, O., Javaheri, A., Auger, A., Bouchard, N., Kron, S. J., Jackson, S. P., and Cote, J. (2004). Binding of chromatin-modifying activities to phosphorylated histone H2A at DNA damage sites. Mol. Cell *16*, 979–990.

Elder, R. T., LOH, E. Y., and Davis, R. W. (1983). RNA from the yeast transposable element Ty1 has both ends in the direct repeats, a structure similar to retrovirus RNA. Proc. Natl. Acad. Sci. USA *80*, 2432–2436.

Gomez, E. B., Espinosa, J. M., and Forsburg, S. L. (2005). Schizosaccharomyces pombe mst2+ encodes a MYST family histone acetyltransferase that negatively regulates telomere silencing. Mol. Cell. Biol. *25*, 8887–8903.

Grant, P. A., Sterner, D. E., Duggan, L. J., Workman, J. L., and Berger, S. L. (1998). The SAGA unfolds: convergence of transcription regulators in chromatin-modifying complexes. Trends Cell Biol. *8*, 193–197.

Grimm, C., Schaer, P., Munz, P., and Kohli, J. (1991). The strong *ADH1* promoter stimulates mitotic and meiotic recombination at the *ADE6* gene of *Schizosaccharomyces pombe*. Mol. Cell. Biol. *11*, 289–298.

Gutz, H. (1971). Site specific induction of gene conversion in *Schizosaccharomyces pombe*. Genetics *69*, 317–337.

Gutz, H., Heslot, H., Leupold, U., and Loprieno, N. (1974). *Schizosaccharomyces pombe*. In: Handbook of Genetics, Vol. 1, ed. R. D. King, New York: Plenum, 395–446.

Hirota, K., Hasemi, T., Yamada, T., Mizuno, K. I., Hoffman, C. S., Shibata, T., and Ohta, K. (2004). Fission yeast global repressors regulate the specificity of chromatin alteration in response to distinct environmental stresses. Nucleic Acids Res. *32*, 855–862.

Hirota, K., Hoffman, C. S., and Ohta, K. (2006). Reciprocal nuclear shuttling of two antagonizing Zn finger proteins modulates Tup family corepressor function to repress chromatin remodeling. Eukaryot. Cell *5*, 1980–1989.

Hirota, K., Hoffman, C. S., Shibata, T., and Ohta, K. (2003). Fission yeast Tup1-like repressors repress chromatin remodeling at the *fbp1*(+) promoter and the *ade6–M26* recombination hotspot. Genetics *165*, 505–515.

Iino, Y., and Yamamoto, M. (1985). Negative control for the initiation of meiosis in *Schizosaccharomyces pombe*. Proc. Natl. Acad. Sci. USA *82*, 2447–2451.

Isshiki, T., Mochizuki, N., Maeda, T., and Yamamoto, M. (1992). Characterization of a fission yeast gene, gpa2, that encodes a G alpha subunit involved in the monitoring of nutrition. Genes Dev. *6*, 2455–2462.

Kon, N., Krawchuk, M. D., Warren, B. G., Smith, G. R., and Wahls, W. P. (1997). Transcription factor Mts1/Mts2 (Atf1/Pcr1, Gad7/Pcr1) activates the M26 meiotic recombination hotspot in *Schizosaccharomyces pombe*. Proc. Natl. Acad. Sci. USA *94*, 13765–13770.

Krebs, J. E., Kuo, M. H., Allis, C. D., and Peterson, C. L. (1999). Cell cycle-regulated histone acetylation required for expression of the yeast HO gene. Genes Dev. *13*, 1412–1421.

Lichten, M., and Goldman, A. S. (1995). Meiotic recombination hotspots. Annu. Rev. Genet. *29*, 423–444.

McLeod, M., and Beach, D. (1986). Homology between the *ran1*+ gene of fission yeast and protein kinases. EMBO J. *5*, 3665–3671.

Mizuno, K., Emura, Y., Baur, M., Kohli, J., Ohta, K., and Shibata, T. (1997). The meiotic recombination hot spot created by the single-base substitution *ade6–M26* results in remodeling of chromatin structure in fission yeast. Genes Dev. *11*, 876–886.

Moreno, S., Klar, A., and Nurse, P. (1991). Molecular genetic analysis of fission yeast *Schizosaccharomyces pombe*. Methods Enzymol. *194*, 795–823.

Nachman, M. W. (2002). Variation in recombination rate across the genome: evidence and implications. Curr. Opin. Genet. Dev. *12*, 657–663.

Nicolas, A. (1998). Relationship between transcription and initiation of meiotic recombination: toward chromatin accessibility. Proc. Natl. Acad. Sci. USA *95*, 87–89.

Ohta, K., Shibata, T., and Nicolas, A. (1994). Changes in chromatin structure at recombination initiation sites during yeast meiosis. EMBO J. *13*, 5754–5763.

Orphanides, G., and Reinberg, D. (2000). RNA polymerase II elongation through chromatin. Nature *407*, 471–475.

Petes, T. D. (2001). Meiotic recombination hot spots and cold spots. Nat. Rev. Genet. *2*, 360–369.

Ponticelli, A. S., Sena, E. P., and Smith, G. R. (1988). Genetic and physical analysis of the M26 recombination hotspot of *Schizosaccharomyces pombe*. Genetics *119*, 491–497.

Sambrook, J., Fritsch, E. F., and Maniatis, T. (1989). Molecular Cloning: A Laboratory Manual, Cold Spring Harbor, NY: Cold Spring Harbor Laboratory Press.

Schuchert, P., Langsford, M., Kaslin, E., and Kohli, J. (1991). A specific DNA sequence is required for high frequency of recombination in the *ade6* gene of fission yeast. EMBO J. *10*, 2157–2163.

Seo, H., Masuoka, M., Murofushi, H., Takeda, S., Shibata, T., and Ohta, K. (2005). Rapid generation of specific antibodies by enhanced homologous recombination. Nat. Biotechnol. *23*, 731–735.

Sherman, F., Fink, G., and Hicks, J. (1986). Methods in Yeast Genetics: Laboratory Course Manual, Cold Spring Harbor, NY: Cold Spring Harbor Laboratory Press.

Steiner, W. W., Schreckhise, R. W., and Smith, G. R. (2002). Meiotic DNA breaks at the *S. pombe* recombination hot spot *M26*. Mol. Cell *9*, 847–855.

Sun, H., Treco, D., Schultes, N. P., and Szostak, J. W. (1989). Double-strand breaks at an initiation site for meiotic gene conversion. Nature *338*, 87–90.

Szankasi, P., Heyer, W. D., Schuchert, P., and Kohli, J. (1988). DNA sequence analysis of the *ade6* gene of *Schizosaccharomyces pombe*. Wild-type and mutant alleles including the recombination host spot allele ade6–M26. J. Mol. Biol. *204*, 917–925.

Takeda, T., and Yamamoto, M. (1987). Analysis and *in vivo* disruption of the gene coding for calmodulin in *Schizosaccharomyces pombe*. Proc. Natl. Acad. Sci. USA *84*, 3580–3584.

Tong, J. K., Hassig, C. A., Schnitzler, G. R., Kingston, R. E., and Schreiber, S. L. (1998). Chromatin deacetylation by an ATP-dependent nucleosome remodelling complex. Nature *395*, 917–921.

Travers, A. (1999). An engine for nucleosome remodeling. Cell *96*, 311–314.

van Attikum, H., Fritsch, O., Hohn, B., and Gasser, S. M. (2004). Recruitment of the INO80 complex by H2A phosphorylation links ATP-dependent chromatin remodeling with DNA double-strand break repair. Cell *119*, 777–788.

Wahls, W. P. (1998). Meiotic recombination hotspots: shaping the genome and insights into hypervariable minisatellite DNA change. Curr. Top. Dev. Biol. *37*, 37–75.

Wahls, W. P., and Smith, G. R. (1994). A heteromeric protein that binds to a meiotic homologous recombination hot spot: correlation of binding and hot spot activity. Genes Dev. *8*, 1693–1702.

Walfridsson, J., Khorosjutina, O., Matikainen, P., Gustafsson, C. M., and Ekwall, K. (2007). A genome-wide role for CHD remodelling factors and Nap1 in nucleosome disassembly. EMBO J. *26*, 2868–2879.

Wolffe, A. (1997). Chromatin: Structure and Function, 3rd ed., San Diego, CA: Academic Press.

Wu, T. C., and Lichten, M. (1994). Meiosis-induced double-strand break sites determined by yeast chromatin structure. Science *263*, 515–518.

Yamada, T., Mizuno, K. I., Hirota, K., Kon, N., Wahls, W. P., Hartsuiker, E., Murofushi, H., Shibata, T., and Ohta, K. (2004). Roles of histone acetylation and chromatin remodeling factor in a meiotic recombination hotspot. EMBO J. *23*, 1792–1803.

Yamamoto, M., Imai, Y., and Watanabe, Y. (1997). Mating and Sporulation in *Schizosaccharomyces pombe*. In: The Molecular and Cellular Biology of the Yeast *Saccharomyces*, ed. J. R. Prigle, J. R. Broach, and E. W. Jones, Cold Spring Harbor, NY: Cold Spring Habor Laboratory Press, 1037–1106.

Yoo, E. J., Jin, Y. H., Jang, Y. K., Bjerling, P., Tabish, M., Hong, S. H., Ekwall, K., and Park, S. D. (2000). Fission yeast hrp1, a chromodomain ATPase, is required for proper chromosome segregation and its overexpression interferes with chromatin condensation. Nucleic Acids Res. *28*, 2004–2011.

Zaman, Z., Ansari, A. Z., Koh, S. S., Young, R., and Ptashne, M. (2001). Interaction of a transcriptional repressor with the RNA polymerase II holoenzyme plays a crucial role in repression. Proc. Natl. Acad. Sci. USA *98*, 2550–2554.

Zhang, Y., LeRoy, G., Seelig, H. P., Lane, W. S., and Reinberg, D. (1998). The dermatomyositis-specific autoantigen Mi2 is a component of a complex containing histone deacetylase and nucleosome remodeling activities. Cell *95*, 279–289.